X-ray spectroscopies on transition metal oxide based catalysts and battery materials

Zhiwei Hu[#], Liu Hao Tjeng[##]

During the last three years our department has started to put substantial effort to study transition metal oxide based catalysts and battery materials using synchrotron radiation. Our objective is to determine the local electronic states of the transition metal ions during the various steps of the operational process. Here we made use of our long-time expertise in soft and hard x-ray absorption spectroscopy: expertise not only in how to experimentally obtain reliable data but especially in how to analyze the spectra in terms of configuration-interaction calculations that include the full atomic multiplet theory, in combination also with our extensive database of reference spectra. We collaborated closely with external partners who are specialists in catalyst and battery research. We selected the systems based on our experience and expectations with transition metal compounds, and in most of the times we were indeed able to extract detailed information concerning the charge (valence), orbital, and/or spin state of the ions. Our research efforts in this field have resulted in more than 40 publications in the 2018-2021 census period; 26 of them are in journals with IF ≥ 12, see our references [1-26].

A project that perhaps illustrates best our ambitions is our ***in-operando*** **soft x-ray absorption spectroscopic study on a Co catalyst** (Jing Zhou, Linjuan Zhang, Yu-Cheng Huang, Chung-Li Dong, Hong-Ji Lin, Chien-Te Chen, Liu Hao Tjeng, and Zhiwei Hu [22]).

We have carried out in the recent past extensive investigations to the electronic structure of many cobalt oxide based solid state materials, see for example refs. [27-35]. These materials have generated considerable attention in the scientific community due to their complex and large diversity of physical phenomena, such as metal-insulator transitions, superconductivity, large magnetoresistance, and high thermoelectric power. This richness of electronic and magnetic properties is closely related not only to the possibility of stabilizing cobalt in different valence states (2+, 3+, and 4+) but also to the so-called spin-state degree of freedom. For example, in an octahedral coordination, Co^{3+} and Co^{4+} ions, which have the formal d^6 and d^5 configurations, respectively, can exist in three possible spin states: a high-spin (HS) state, a low-spin (LS) state, and even an intermediate-spin (IS) state. We were quite successful in determining the charge, spin, and orbital states of many of these complex cobalt oxide materials [27-35], and we were therefore ready to take up the challenge to investigate the electronic structure of Co oxides that are being utilized in catalytic processes. In particular, we would like to utilize soft x-ray absorption spectroscopy since this is our main method by which we were able to determine the charge, spin, and orbital states successfully.

To identify the active sites and the reaction mechanism in a catalytic process, it is highly desirable to determine the local electronic structure of the participating ions *during* the electrochemical reaction. To carry out such an *in-operando* soft x-ray experiment is, however, far from trivial. It is a major challenge to overcome the limitations set by the extremely short mean free paths of the soft x-rays and various other signals that are representative for the absorption process. Nevertheless, we have succeeded in constructing a device that allows such an *in-operando* soft x-ray experiment. The device is described below in the **Experimental Method** section.

In figure (a) below, we present the O–*K* spectra of $Li_2Co_2O_4$ *in-operando* as a function of the number of scans (taken within 2 min for each scan) at an applied voltage of 1.6 V. One can clearly observe that the spectral intensities of peaks labelled as β and γ increase quickly at the expense of peak α, and reached a steady-state value after 20 min. In figure (b) on page 2, we show the steady-state spectra as a function of applied voltage. The inset displays the cycle voltammograms of $Li_2Co_2O_4$, revealing that the material becomes fully OER active at 1.6 V.

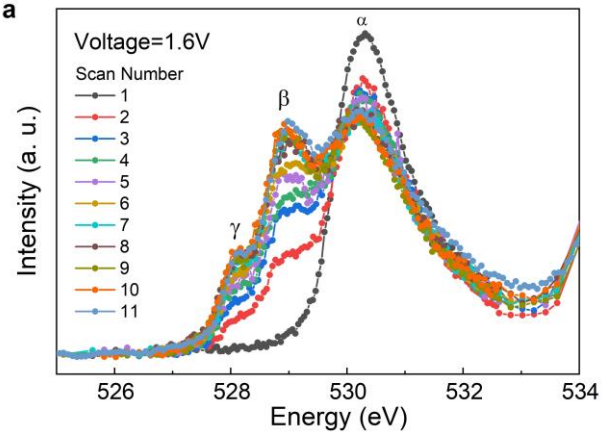

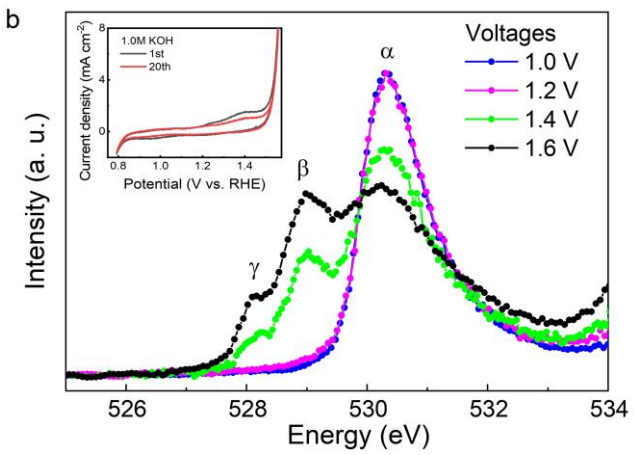

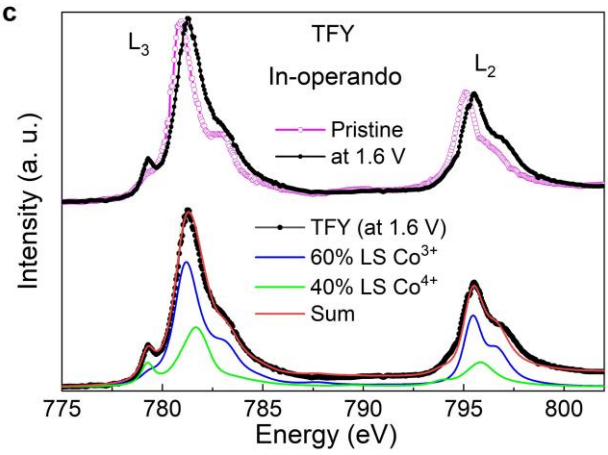

To interpret the spectra, we make use of our extensive database, which include spectra of $Li_{0.66}CoO_2$ ($Co^{3.34+}$), $Na_{0.5}CoO_2$ ($Co^{3.5+}$), and $BaCoO_3$ (LS Co^{4+}). The single peak α in the spectrum of pristine $Li_2Co_2O_4$ can be assigned to a transition from the O 1*s* core level to the unoccupied 3*d*-e_g state of a LS Co^{3+}, while the two additional peaks β and γ at lower energies are due to transitions to the unoccupied 3*d*-t_{2g} and 3*d*-e_g orbitals of a LS Co^{4+} ion, respectively.

The increase in the spectral intensities of the β and γ features during the OER thus indicates that there is a transition from a Co^{3+} state to a Co^{4+} state in the $Li_2Co_2O_4$ catalyst during the electrochemical reaction. The Co^{4+} content can be estimated by constructing a weighted sum of the spectrum of pristine $Li_2Co_2O_4$ and that of $BaCoO_3$. We obtained a $Co^{3.4+}$ valence state in $Li_2Co_2O_4$ under an applied voltage of 1.6 V and $Co^{3.2+}$ at 1.4 V. Below an applied voltage of 1.4 V there is no Co^{4+} and the material is not OER active as shown in the cycle voltammograms (inset of figure b).

We have carried out further measurements, after the OER, at the O-*K* edge using the *in-vacuo* total electron yield method (TEY) which is much more surface sensitive, and found the same steady-state spectrum as with TFY during OER. This confirms that the TFY signal is representative for the active region for the OER reaction. In the Experimental Method section we can provide a quantitative estimate that ~80% of the TFY signal originates indeed from this region.

To double check our findings, we have also carried out measurements at the Co-$L_{2,3}$ edge using the *in-operando* TFY. The figure (c) on the top right shows that there is a shift in the Co-$L_{2,3}$ spectrum towards higher energies when comparing the $Li_2Co_2O_4$ under OER condition (1.6 V applied voltage) with the as-prepared $Li_2Co_2O_4$ (pristine), indicating again an increase in the Co valence. We have also quantitatively analyzed these spectra in terms of a weighted sum of the theoretical LS Co^{3+} and LS Co^{4+} spectra. We found 60% Co^{3+} and 40% $Co^{4+,}$ i.e., an LS $Co^{3.4+}$ state, which is fully consistent with the O–*K* data.

To summarize, our *in-operando* soft x-ray absorption measurements demonstrate that a substantial fraction of the Co ions undergoes a voltage-dependent and time-dependent valence state transition from Co^{3+} to Co^{4+}. A delithiation process is thus taking place. Since we have not detected the presence of any IS Co^{3+} species in our spectra, we infer that it is the highly oxidized Co^{4+} site, rather than the Co^{3+} site or perhaps the oxygen vacancy site, that is mainly responsible for the high OER activity. It is exciting that our findings contradict the commonly accepted IS Co^{3+} or $(e_g)^1$ scenarios but further research on other systems will be needed.

Experimental Method:

The *in-operando* soft x-ray absorption spectroscopy (XAS) experiments at the O–*K* and Co-$L_{2,3}$ edges were carried out at the 11A beam line of the National Synchrotron Radiation Research Center in Taiwan using the total fluorescence yield (TFY) mode. NiO and CoO single crystals were recorded simultaneously in a separate ultrahigh vacuum chamber to serve as energy references for the O–*K* and Co-$L_{2,3}$ edges, respectively.

The $Li_2Co_2O_4$ catalyst powder was dispersed in ethanol and deionized water and then sonicated for 30 min. The ink was dropped into a thin membrane window (100 nm silicon nitride with a 1 × 1 mm^2 area coated by 3 nm Ti/10 nm Au from Silson Ltd) with a loading mass of ~1 mg cm^{-2}. This window was used as the working electrode and to separate the liquid and the ultrahigh vacuum environment. The experiments were performed using an in situ electrochemical liquid cell equipped with three electrodes (working, reference, and counter electrodes) under control by a VersaSTAT 3 potentiostat from Princeton Applied Research. Two

platinum wires were used as the reference and counter electrodes. Here, we selected a Pt pseudoreference electrode due to space constrictions in the electrochemical cell and calibrated the potential to RHE following the Kasem-Jones procedure. Freshly prepared O_2-saturated 1.0 M KOH was used as the electrolyte, and the electrochemical liquid cell system also contained a liquid pump, an inlet, and an outlet tube for the electrolyte flow. All electrode potentials were referred to RHE.

TFY was used as the detection method for the absorption signal in the XAS experiments. A photon escape depth of ~200 nm is sufficiently large to overcome the liquid region and the membrane separating the liquid from the ultrahigh vacuum. The particle size and distribution of $Li_2Co_2O_4$ nanoparticles used in the experiments were determined by high-resolution transmission electron microscopy. The average size of particles was < 20 nm, which ensures sensitivity to the surface region of the catalyst material in the XAS measurements. Assuming that the active region for the OER reaction is within a depth of ~5 nm from the surface, it can be estimated that ~80% of the TFY signal originates from this region.

External Cooperation Partners

Chien-Te Chen, Chih-Wen Pao, and Hong-Ji Lin (National Synchrotron Radiation Research Center (NSRRC), Hsinchu, Taiwan); Chung-Li Dong and Yu-Cheng Huang (Department of Physics, Tamkang University, Tamsui 25137, Taiwan); Jing Zhou, Linjuan Zhang and Jian-Qiang Wang (Shanghai Institute of Applied Physics, Chinese Academy of Sciences, Shanghai 201800, China); Xiaoqing Huang (College of Chemistry, Chemical Engineering and Materials Science, Soochow University, Jiangsu, 215123, China); Wei Zhou and Zongping Shao (College of Chemical Engineering, Nanjing Tech University, Nanjing 211800, P. R. China and Department of Chemical Engineering, Curtin University, Perth, Western Australia 6845, Australia.)

References

(references with * are listed in descending IF order)

[1]* *High-performance diluted nickel nanoclusters decorating ruthenium nanowires for pH-universal overall water splitting, T. Zhu, S. Liu, B. Huang, Q. Shao, M. Wang, F. Li, X. Tan, Y. Pi, S.-C. Weng, B. Huang, Z. Hu et al., Energy Environ. Sci. (2021), doi.org/10.1039/d0ee04028b*

[2]* *A Universal Strategy to Design Superior Water-Splitting Electrocatalysts Based on Fast In Situ Reconstruction of Amorphous Nanofilm Precursors, C. Gao, Z. Hu, Y. Zhu, B. Gu, Y. Zhong, H.-J. Lin, C.-T. Chen, W. Zhou, and Z. Shao, Adv. Mater. **30** (2018) 1804333, doi.org/10.1002/adma.201804333*

[3]* *An Amorphous Nickel–Iron-Based Electrocatalyst with Unusual Local Structures for Ultrafast Oxygen Evolution Reaction, G. Chen, Y. Zhu, H. M. Chen, Z. Hu, S.-F. Hung, N. Ma, J. Dai, H.-J. Lin, C.-T. Chen, W. Zhou, and Z. Shao, Adv. Mater. **31** (2019) 1900883, doi.org/10.1002/adma.201900883*

[4]* *Boosting Oxygen Evolution Reaction by Creating Both Metal Ion and Lattice-Oxygen Active Sites in a Complex Oxide, Y. Zhu, H. A. Tahini, Z. Hu, Z.-G. Chen, W. Zhou, A. C. Komarek, Q. Lin, H.-J. Lin, C.-T. Chen, Y. Zhong et al., Adv. Mater. **32** (2019) 1905025, doi.org/10.1002/adma.201905025*

[5]* *Li-Ti Cation Mixing Enhanced Structural and Performance Stability of Li-Rich Layered Oxide, S. Liu, Z. Liu, X. Shen, X. Wang, S.-C. Liao, R. Yu, Z. Wang, Z. Hu, C.-T. Chen, X. Yu et al., Adv. Energy Mater. **9** (2019) 1901530, doi.org/10.1002/aenm.201901530*

[6]* *Eliminating Transition Metal Migration and Anionic Redox to Understand Voltage Hysteresis of Lithium-Rich Layered Oxides, M. Han, J. Jiao, Z. Liu, X. Shen, Q. Zhang, H.-J. Lin, C.-T. Chen, Q. Kong, W. K. Pang, Z. Guo et al., Adv. Energy Mater. **10** (2020) 1903634, doi.org/10.1002/aenm.201903634*

[7]* *High-Index Faceted RuCo Nanoscrews for Water Electrosplitting, T. Zhu, J. Huang, B. Huang, N. Zhang, S. Liu, Q. Yao, S.-C. Haw, Y.-C. Chang, C.-W. Pao, J.-M. Chen et al., Adv. Energy Mater. **10** (2020) 2002860, doi.org/10.1002/aenm.202002860*

[8]* *Stacking Faults Hinder Lithium Insertion in Li_2RuO_3, M. Han, Z. Liu, X. Shen, L. Yang, X. Shen, Q. Zhang, X. Liu, J. Wang, H.-J. Lin, C.-T. Chen et al., Adv. Energy Mater. **10** (2020) 2002631, doi.org/10.1002/aenm.202002631*

[9]* *A molecular-level strategy to boost the mass transport of perovskite electrocatalyst for enhanced oxygen evolution, S. She, Y. Zhu, H. A. Tahini, Z. Hu, S.-C. Weng, X. Wu, Y. Chen, D. Guan, Y. Song, J. Dai et al., Appl. Phys. Rev. **8** (2021) 011407, doi.org/10.1063/5.0033912*

[10]* *Searching General Sufficient-and-Necessary Conditions for Ultrafast Hydrogen-Evolving Electrocatalysis, D. Guan, J. Zhou, Z. Hu, W. Zhou, X. Xu, Y. Zhong, B. Liu, Y. Chen, M. Xu, H.-J. Lin et al., Adv. Funct. Mater. **29** (2019) 1900704, doi.org/10.1002/adfm.201900704*

[11]* *Single-Atom In-Doped Subnanometer Pt Nanowires for Simultaneous Hydrogen Generation and Biomass Upgrading, Y. Zhu, X. Zhu, L. Bu, Q. Shao, Y. Li, Z. Hu, C.-T. Chen, C.-W. Pao, S. Yang, and X. Huang, Adv. Funct. Mater. **30** (2020) 2004310, doi.org/10.1002/adfm.202004310*

[12]* *Selective Surface Reconstruction of a Defective Iridium-Based Catalyst for High-Efficiency Water Splitting, Y. Pi, Y. Xu, L. Li, T. Sun, B. Huang, L. Bu, Y. Ma, Z. Hu, C.-W. Pao, and X. Huang, Adv. Funct. Mater. **30** (2020) 2004375, doi.org/10.1002/adfm.202004375*

[13]* *Superiority of native vacancies in activating anionic redox in P2-type $Na_{2/3}[Mn_{7/9}Mg_{1/9}\square_{1/9}]O_2$, L. Yang, Z. Liu, S. Liu, M. Han, Q. Zhang, L. Gu, Q. Li, Z. Hu, X. Wang, H.-J. Lin et al., Nano Energy **78** (2020) 105172, doi.org/10.1016/j.nanoen.2020.105172*

[14]* *Vitalization of P2–$Na_{2/3}Ni_{1/3}Mn_{2/3}O_2$ at high-voltage cyclability via combined structural modulation for sodium-ion batteries*, Y. Huang, Z. Yan, W. Luo, Z. Hu, G. Liu, L. Zhang, X. Yang, M. Ou, W. Liu, L. Huang et al., *Energy Stor. Mater.* ***29*** *(2020) 182,* doi.org/10.1016/j.ensm.2020.04.012

[15]* *Deciphering the Interface of a High-Voltage (5 V-Class) Li-Ion Battery Containing Additive-Assisted Sulfolane-Based Electrolyte*, D. Lu, G. Xu, Z. Hu, Z. Cui, X. Wang, J. Li, L. Huang, X. Du, Y. Wang, J. Ma et al., *Small Methods* ***3*** *(2019) 1900546,* doi.org/10.1002/smtd.201900546

[16]* *Surface-Regulated Rhodium–Antimony Nanorods for Nitrogen Fixation*, N. Zhang, L. Li, J. Wang, Z. Hu, Q. Shao, X. Xiao, and X. Huang, *Angew. Chem. Int. Ed.* ***59*** *(2020) 8066,* doi.org/10.1002/anie.201915747

[17]* *Highly Reversible Cuprous Mediated Cathode Chemistry for Magnesium Batteries*, X. Cheng, Z. Zhang, Q. Kong, Q. Zhang, T. Wang, S. Dong, L. Gu, X. Wang, J. Ma, P. Han et al., *Angew. Chem. Int. Ed.* ***59*** *(2020) 11477,* doi.org/10.1002/anie.202002177

[18]* *Partially Pyrolyzed Binary Metal–Organic Framework Nanosheets for Efficient Electrochemical Hydrogen Peroxide Synthesis*, M. Wang, N. Zhang, Y. Feng, Z. Hu. Q. Shao, and X. Huang, *Angew. Chem. Int. Ed.* ***59*** *(2020) 14373,* doi.org/10.1002/anie.202006422

[19]* *Mg-Pillared $LiCoO_2$: Towards Stable Cycling at 4.6 V*, Y. Huang, Y. Zhu, H. Fu, M. Ou, C. Hu, S. Yu, Z. Hu, C.-T. Chen, G. Jiang, H. Gu et al., *Angew. Chem. Int. Ed.* ***60*** *(2020) 4682,* doi.org/10.1002/anie.202014226

[20]* *An Efficient Interfacial Synthesis of Two-Dimensional Metal-Organic Framework Nanosheets for Electrochemical Hydrogen Peroxide Production*, M. Wang, X. Dong, Z. Meng, Z. Hu, Y.-G. Lin, C.-K. Peng, H. Wang, C.-W. Pao, S. Ding, Y. Li et al., *Angew. Chem. Int. Ed.* ***60*** *(2021) 11190,* doi.org/10.1002/anie.202100897

[21]* *Unusual synergistic effect in layered Ruddlesden - Popper oxide enables ultrafast hydrogen evolution*, Y. Zhu, H. A. Tahini, Z. Hu, J. Dai, Y. Chen, H. Sun, W. Zhou, M. Liu, S. C. Smith, H. Wang and Z. Shao, *Nat. Commun.* ***10*** *(2019) 149,* doi.org/10.1038/s41467-018-08117-6

[22]* *Voltage- and time-dependent valence state transition in cobalt oxide catalysts during the oxygen evolution reaction*, J. Zhou, L. Zhang, Y.-C. Huang, C.-L. Dong, H.-J. Lin, C.-T. Chen. L. H. Tjeng and Z. Hu, *Nat. Commun.* ***11*** *(2020) 1984,* doi.org/10.1038/s41467-020-15925-2

[23]* *Utilizing ion leaching effects for achieving high oxygen-evolving performance on hybrid nanocomposite with self-optimized behaviors*, D. Guan, G. Ryu, Z. Hu, J. Zhou, C.-L. Dong, Y.-C. Huang, K. Zhang, Y. Zhong, A. C. Komarek, M. Zhu et al., *Nat. Commun.* ***11*** *(2020) 3376,* doi.org/10.1038/s41467-020-17108-5

[24]* *Single-phase perovskite oxide with super-exchange induced atomic-scale synergistic active centers enables ultrafast hydrogen evolution*, J. Dai, Y. Zhu, H. A. Tahini, Q. Lin, Y. Chen, D. Guan, C. Zhou, Z. Hu, H.-J. Lin, T.-S. Chan et al., *Nat. Commun.* ***11*** *(2020) 5657,* doi.org/10.1038/s41467-020-19433-1

[25]* *In-situ visualization of the space-charge-layer effect on interfacial lithium-ion transport in all-solid-state batteries*, L. Wang, R. Xie, B. Chen, X. Yu, J. Ma, C. Li, Z. Hu, X. Sun, C. Xu, S. Dong et al., *Nat. Commun.* ***11*** *(2020) 5889,* doi.org/10.1038/s41467-020-19726-5

[26]* *Fast operando spectroscopy tracking in situ generation of rich defects in silver nanocrystals for highly selective electrochemical CO_2 reduction*, X. Wu, Y. Guo, Z. Sun, F. Xie, D. Guan, J. Dai, F. Yu, Z. Hu, Y.-C. Huang, C.-W. Pao et al., *Nat. Commun.* ***12*** *(2021) 660,* doi.org/10.1038/s41467-021-20960-8

[27] *Different Look at the Spin State of Co^{3+} Ions in a CoO_5 Pyramidal Coordination*, Z. Hu, H. Wu, M. W. Haverkort, H. H. Hsieh, H.-J. Lin, T. Lorenz, J. Baier, A. Reichl, I. Bonn, C. Felser et al., *Phys. Rev. Lett.* ***92*** *(2004) 207402,* doi.org/10.1103/PhysRevLett.92.207402

[28] *Nature of Magnetism in $Ca_3Co_2O_6$*, H. Wu, M. W. Haverkort, Z. Hu, D. I. Khomskii, and L. H. Tjeng, *Phys. Rev. Lett.* ***95*** *(2005) 186401,* doi.org/10.1103/PhysRevLett.95.186401

[29] *Controlling Orbital Moment and Spin Orientation in CoO Layers by Strain*, S. I. Csiszar, M. W. Haverkort, Z. Hu, A. Tanaka, H. H. Hsieh, H.-J. Lin, C. T. Chen, T. Hibma, and L. H. Tjeng, *Phys. Rev. Lett.* ***95*** *(2005) 187205,* doi.org/10.1103/PhysRevLett.95.187205

[30] *Spin State Transition in $LaCoO_3$ Studied Using Soft X-ray Absorption Spectroscopy and Magnetic Circular Dichroism*, M. W. Haverkort, Z. Hu, J. C. Cezar, T. Burnus, H. Hartmann, M. Reuther, C. Zobel, T. Lorenz, A. Tanaka, N. B. Brookes et al., *Phys. Rev. Lett.* ***97*** *(2006) 176405.*

[31] *Ising Magnetism and Ferroelectricity in Ca_3CoMnO_6*, H. Wu, T. Burnus, Z. Hu, C. Martin, A. Maignan, J. C. Cezar, A. Tanaka, N. B. Brookes, D. I. Khomskii, and L. H. Tjeng, *Phys. Rev. Lett.* ***102*** *(2009) 026404,* doi.org/10.1103/PhysRevLett.102.026404

[32] *Spin blockade, orbital occupation, and charge ordering in $La_{1.5}Sr_{0.5}CoO_4$*, C. F. Chang, Z. Hu, H. Wu, T. Burnus, N. Hollmann, M. Benomar, T. Lorenz, A. Tanaka, H.-J. Lin, H. H. Hsieh et al., *Phys. Rev. Lett.* ***102*** *(2009) 116401.*

[33] *Determination of the Co Valence in Bilayer Hydrated Superconducting $Na_xCoO_2{\cdot}yH_2O$ by Soft X-Ray Absorption Spectroscopy*, H. Ohta, K. Yoshimura, Z. Hu, Y. Y. Chin, H.-J. Lin, H. H. Hsieh, C. T. Chen, and L. H. Tjeng, *Phys. Rev. Lett.* ***107*** *(2011) 066404,* doi.org/10.1103/PhysRevLett.107.066404

[34] *A Complete High-to-Low spin state Transition of Trivalent Cobalt Ion in Octrahedral Symmetry in $SrCo_{0.5}Ru_{0.5}O_3$*, J.-M. Chen, Y.-Y. Chin, M. Valldor, Z. Hu, J.-M. Lee, S.-C. Haw, N. Hiraoka, H. Ishii, C.-W. Pao, K.-D. Tsuei et al., *J. Am. Chem. Soc.* ***136*** *(2014) 1514,* doi.org/10.1021/ja4114006

[35] *Origin of Ising magnetism in $Ca_3Co_2O_6$ unveiled by orbital imaging*, B. Leedahl, M. Sundermann, A. Amorese, A. Severing, H. Gretarsson, L. Zhang, A. C. Komarek, A. Maignan, M. W. Haverkort, and L. H. Tjeng, *Nat. Commun.* ***10*** *(2019) 5447,* doi.org/10.1038/s41467-019-13273-4

[#] zhiwei.hu@cpfs.mpg.de
[##] hao.tjeng@cpfs.mpg.de